The Kinetics and Formation of Small Carbon Clusters in an Argon Matrix

Jan Szczepanski, Robert Pellow, and Martin Vala

Department of Chemistry, University of Florida, Gainesville, Florida, USA

Z. Naturforsch. **47a**, 595–604 (1992); received November 25, 1991

Pure carbon clusters, formed by Nd/YAG laser ablation of graphite, have been trapped in an argon matrix at 12 K. The temperature dependence of the prominent infrared absorption bands attributable to C_3, C_5, C_6, and C_9 clusters has been investigated between 12 K and 38 K. The former two are observed to decay and the latter two to grow with increased matrix annealing. A new kinetic model based on solid state diffusion theory and involving thermally activated diffusion and aggregation is introduced. All possible pairwise interactions of the linear carbon clusters from C_1 to C_{10} are included in the model. The coupled differential equations are solved numerically and provide a reasonable fit to the experimental temperature profiles of the known clusters. Predictions emerge from the fit for the unknown matrix infrared frequencies for the C_7 cluster. On the basis of the predicted concentration invariance with temperature for C_7, the infrared bands at 2128 cm^{-1} and 1894 cm^{-1} are ascribed to this linear cluster. This attribution supports the recent assignment of the gaseous 2138 cm^{-1} band to linear C_7.

I. Introduction

Carbon clusters have attracted much attention recently because of their probable importance in certain aspects of astrophysics, soot formation and flame chemistry [1]. Carbon vaporized from graphite and trapped in a cryogenic rare gas matrix displays numerous infrared bands in the carbon-carbon stretching region indicating the presence of many absorbing species, i.e. different carbon clusters [2–5]. It has been known for some time [2] that annealing the matrix can cause the relative intensities of bands either to decrease, to increase, to disappear or to appear for the first time. While growth (or decay) patterns of some bands have been reported in the literature [2–5], no systematic study of their behavior with temperature has been reported. For such a study to succeed, the infrared bands must be conclusively attributed to specific clusters. Previously this would not have been possible, but now, through the combined efforts of matrix isolation and vapor phase investigation in concert with theoretical studies, a number of IR assignments are becoming firmed up. Recent developments are briefly reviewed here. In the present paper we report on the growth and decay of the major small ($n \leq 9$) linear carbon clusters as a function of matrix annealing. In addition, a new kinetic model is introduced which accounts reasonably well for the observed growth and decay patterns.

Spectroscopic kinetic studies of the formation of small clusters have not been numerous [6–11]. Yamada, Usui, and Takagi [6] and Castleman and Keesee [7] investigated the kinetics and formation of metal clusters during expansion through a nozzle. In each case a model built on classical nucleation theory was utilized to extract information on cluster formation. Bernholc and Phillips simulated gas-phase carbon cluster aggregation for neutral and charged clusters [8]. The Smoluchowski equations were solved using electronic structure calculations to obtain the needed kinetic parameters. Good agreement with experimental data was achieved. Ozin and Huber used a simplified version of the Smoluchowski diffusion-controlled kinetic theory to explain their photoaggregation results for small Ag clusters in argon matrices [9]. Moskovits and Hulse introduced a quenched reaction model [10] in which successive additions of monomer (or ligand) to the growing cluster (complex) were considered. Applied to the formation of $Ni_x(CO)_y$ complex clusters, the model was shown to give an acceptable fit to the data. Nishiya et al. extended the quenched reaction model to include new channels for cluster formation (addition of dimers and trimers) in their IR study of ammonia clusters [11]. In the present work we adopt the full Smoluchowski diffusion-controlled kinetic model [12] and allow for the formation of linear carbon

Reprint requests to Prof. M. Vala, Department of Chemistry, University of Florida, Gainesville, FL 32611-2046/USA

0932-0784 / 92 / 0400-0595 $ 01.30/0. – Please order a reprint rather than making your own copy.

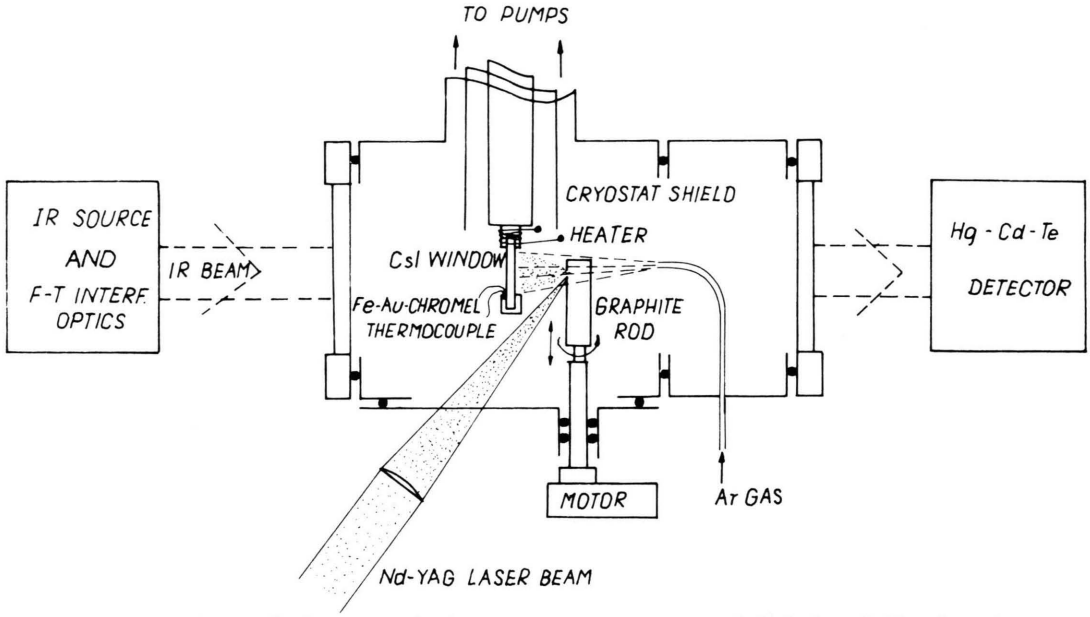

Fig. 1. Experimental setup for laser vaporization of graphite rod and matrix isolation of ablated species.

clusters via all possible routes (i. e., addition of monomers, dimers, trimers, etc.).

The paper is arranged as follows. The experimental details are described in Section II. A brief review of the current state of knowledge of the IR assignments of the small carbon clusters is given in Section III. In Section IV, the annealing results are presented (IVA), followed by some possible limitations on aggregation reactions (IVB) and then a description of the carbon cluster reaction model (IVC). Section IVD gives details on the computational approach used and, finally, the results are discussed in Section V.

II. Experimental

The apparatus and procedures used have been described previously[13], so only a brief description is given here. The carbon clusters were produced by laser ablation of graphite using a slightly focussed Q-switched Nd/YAG laser (Spectra Physics, DCR-11, 532 nm, 1.0 mJ/pulse, 10 Hz rep. rate). A schematic of the vaporization/deposition cell is shown in Figure 1. The ablated graphite products were trapped with argon (99.995% pure, Matheson) at 12 K on a CsI window mounted on the cold finger of a closed-cycle helium cryostat (Displex DE 202, APD). Under similar conditions, both ESR[14] and previous IR[4,13] measurements have shown that large quantities of C_3, C_5, and C_6 clusters are produced and trapped.

Infrared spectra were obtained on a Nicolet FTIR spectrometer using 200 scans with 1 cm^{-1} resolution. After a scan at 12 K, the matrix was annealed for 10 min at an elevated temperature (from 23 to 38 K), then returned to 12 K where another spectrum was collected. This procedure was then repeated at a higher annealing temperature.

III. Review of Carbon Cluster IR Assignments

Since one of the major goals of this work is to study the aggregation of carbon clusters in an argon matrix by investigating the temperature dependence of the infrared bands of the clusters, it is imperative that the specific IR bands followed be well-assigned. In this section we give a brief review of the present status of the IR band assignments of the small ($n \leq 9$) carbon clusters, with emphasis on matrix studies. An excellent review through April 1989 has been provided by Weltner and Van Zee[1], but there have been significant advances since then.

A) C_3

Probably the best known of the small clusters, C_3 was studied in matrices using isotopic substitution by

Weltner and coworkers[2,15,16] who proved conclusively that the 2039 cm^{-1} (Ar matrix) band originated from linear C_3.

B) C_4

Using isotopically labelled acetylene, diacetylene and butadiene, Shen and Graham showed[17] that the 1544 cm^{-1} IR band originates from linear C_4. Laser ablation studies have not been successful in producing intense enough bands in this region to discern isotopomeric structure[18].

C) C_5

An early assignment of the 2164 cm^{-1} Ar matrix band to C_4 was proven to be erroneous, when a laser-vaporized, matrix-deposited 1:1 mixtrue of $^{12}C:^{13}C$ was shown[18] to exhibit twenty isotopomeric peaks. For linear C_4 only 10 peaks are predicted[19]. For C_5, the most reasonable structures and the expected number of isotopomers for each (in parentheses) are trigonal bipyramidal (12), planar cyclic (8) and linear (20). A normal coordinate analysis of the linear form provided strong support[18] for the assignment of the 2164 cm^{-1} band to linear C_5. Soon thereafter, studies of vapor phase C_5 confirmed this assignment[20]. At about the same time, C_5 was discovered[21] in the cool shell of a carbon star by the rotational analysis of the infrared band system at 2169 cm^{-1}.

D) C_6

A prominent band at 1952 cm^{-1} has been shown[4] to exhibit 35 isotopomeric peaks. Thirty-six are expected for linear C_6. Normal coordinate analysis on near-linear C_6 provided strong support for the assignment of this band to cumulenic C_6; of the 36 expected peaks two were found to be overlapped. This assignment has been confirmed by Martin, Francois, and Gijbels using MP2/6-31G* level *ab initio* theoretical calculations[23].

E) C_7

No matrix studies have been reported which provide conclusive evidence for the IR assignment of this species. A very recent vapor phase study by Saykally and co-workers[24] shows that a band at 2138 cm^{-1} results from the linear cumulenic C_7 cluster. In this paper we provide evidence that the 2128 cm^{-1} and 1894 cm^{-1} matrix bands are to C_7 (*vide infra*).

F) C_9

The temperature-sensitive band at 1998 cm^{-1} had been assigned tentatively[4] to C_8. This assignment relied on band density and isotopomeric peak intensity arguments. For linear C_8, 136 isotopomeric peaks are expected[19] in a span of $\sim$78 cm^{-1}. Over one hundred isotopomeric bands built on the 1998 cm^{-1} band were observed, but considerable band overlapping is present. Although this observation clearly rules out in earlier C_6 assignment[2], it is consistent with attribution to *either* a C_8 *or* higher carbon cluster. This assignment to C_8 has been questioned on theoretical grounds by Martin and co-workers[23] who favor a C_9 assignment. Heath and Saykally have observed a gas-phase band at 2014 cm^{-1} which they attribute[25a] to linear C_9. They further suggest[25b] on the basis of a comparison of gas-phase frequencies of C_3, C_5, C_7, and C_9 with certain matrix frequencies that there is a linear gas-to-matrix frequency shift which increases with cluster size and that the 1998 cm^{-1} matrix band should be attributed to C_9. In a recently completed isotopic matrix study[26] in the IR, we have confirmed that the 1998 cm^{-1} band is due to C_9.

IV. Results

A) *Annealing Studies*

The temperature dependence (12 K–36 K) of the infrared spectra of the carbon clusters produced via laser ablation is shown in Figure 2. To emphasize the changes produced upon annealing, the difference spectrum (30 K spectrum minus 12 K spectrum) is shown in Figure 3. The prominent negative bands belong to C_3 (2039 cm^{-1}) and C_5 (2164 cm^{-1}), indicating their diminution upon annealing. The important positive difference bands belong to C_6 (1952 cm^{-1}) and C_9 (1998 cm^{-1}), indicating that they increase upon warming the matrix. While this difference spectrum indicates the overall result of annealing, it does not indicate the detailed changes which occur with each temperature increment. This is provided in Figure 4, where the important IR peak heights are plotted as a function of annealing temperature. C_5 (2164 cm^{-1}) increases slightly up to 23 K and then decreases, more or less in parallel with C_3 (2039 cm^{-1}). C_6

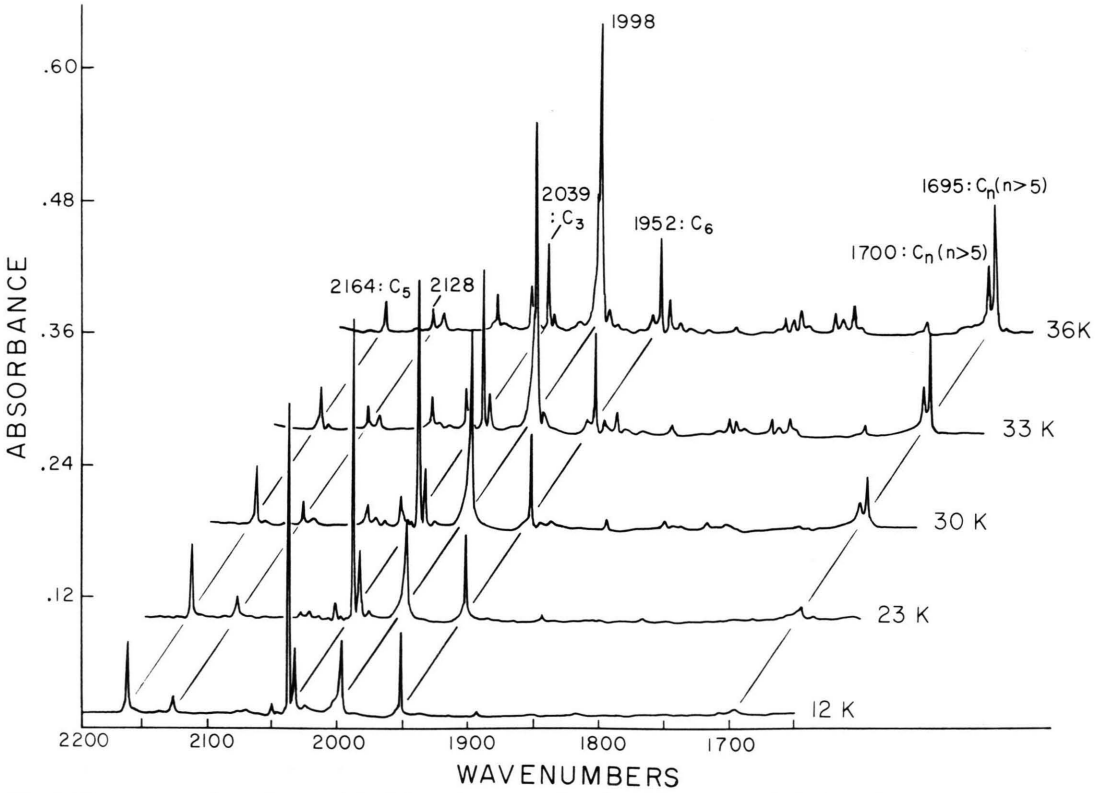

Fig. 2. Temperature dependence of the infrared spectra of carbon clusters matrix-isolated in argon. All spectra were run at 12 K; temperatures denote the annealing temperatures.

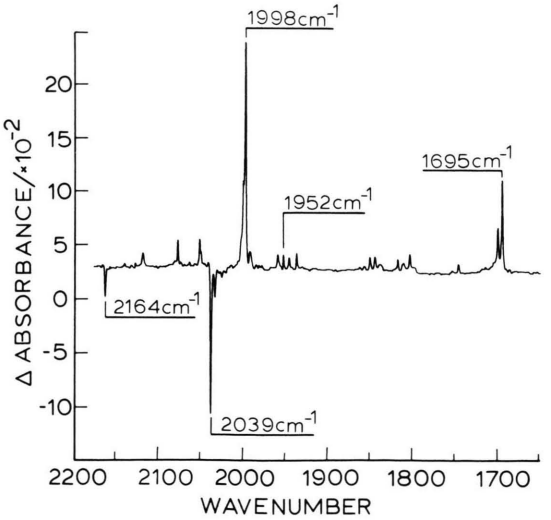

Fig. 3. IR difference spectrum (Annealed-to-30 K spectrum minus nonannealed 12 K one) in an argon marix.

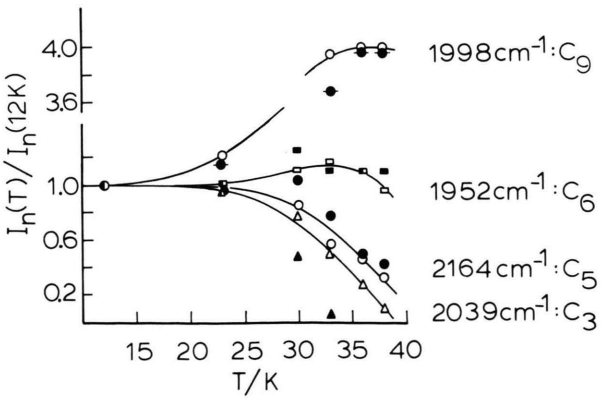

Fig. 4. Temperature vs. IR band peak intensities for specific carbon clusters in an argon matrix. The solid lines are drawn through the (open) experimental data points; the calculated points at the same temperatures are filled (black).

(1952 cm^{-1}) increases up to ~ 33 K and then declines. C_9 (1998 cm^{-1}) increases markedly (factor of ~ 4 greater than C_6) up to 33 K and declines thereafter.

Changes in IR band intensities upon matrix annealing have been observed by previous workers. Thompson, DeKock and Weltner (TDW) suggested [2] that as a result of annealing the C_3 cluster dimerized to form C_6. In our investigation, warming to 33 K caused the 2039 cm^{-1} C_3 peak to decrease to one half its 12 K intensity, while the C_6 peak grew (at 33 K) to only 1.2 times its 12 K intensity and at higher temperatures decreased. Based on these observations, it seems clear that the mechanism for the production of C_6 is more complicated than the simple dimerization of two C_3 clusters. Indeed, given the temperature-dependent behavior for the four known neutral carbon clusters shown in Fig. 4, any realistic model must be able to account for the growth and/or decay of all potentially matrix-mobile species. Such an attempt is made here. Certain limitations on specific clusters' ground state reactivity need to be recognized first, however.

B) *Limitations on Possible Aggregation Reactions*

The specific limitations which need to be considered are 1) decreased diffusional capability as cluster size increases and 2) conservation of spin between reactant and product clusters. In general, the heats of formation of all linear carbon clusters formed from smaller fragments are expected to be greater than 120 kcal/mol and exothermic [27]. The even linear clusters ($n = 4$, 6, 8, 10) are expected [27] (and are observed [14, 28]) to have $^3\Sigma_g^-$ ground states, while the odd clusters are predicted [27] to have $^1\Sigma_g^+$ ground states. Thus, spin-conservation considerations [2] forbid reactions such as

$$2\,C_2(^1\Sigma_g^+) \rightarrow C_4(^3\Sigma_g^-)$$

$$2\,C_{2n-1}(^1\Sigma_g^+) \rightarrow C_{2(2n-1)}(^3\Sigma_g^-), \quad n > 1,$$

$$C_n + C_{n+1} \rightarrow C_{2n+1}, \quad n > 2$$

for all species in their ground electronic states. It may be possible, however, to form the above product clusters via excited product states, the energy provided by the exothermicity of the cluster aggregation. For example, linear C_6 could be formed in the following way

$$C_3(^1\Sigma_g^+) + C_3(^1\Sigma_g^+) \rightarrow C_6(^1\Sigma_g^+), \quad \text{excited state.}$$

Or via other reactant fragments utilizing only ground electronic states

$$C(^3P_g) + C_5(^1\Sigma_g^+) \rightarrow C_6(^3\Sigma_g^-), \quad \text{ground state,}$$

$$C_2(^1\Sigma_g^+) + C_4(^3\Sigma_g^-) \rightarrow C_6(^3\Sigma_g^-), \quad \text{ground state.}$$

C) *Carbon Cluster Reaction Model*

From the above description of the annealing behavior of the known carbon clusters, it is apparent that a simple model, such as one allowing for only carbon atom diffusion in the matrix, would be inadequate. Indeed, it appears that reaction in the matrix occurs for even the largest clusters known (i.e., C_9). We have therefore set up a kinetic model which allows for reaction between all pairwise combinations of cluster species leading to products up through C_{10}. The reaction scheme is diagrammed in Figure 5. There it can be seen, for example, that C_6 may be formed via the reaction of $C + C_5$, $C_2 + C_4$, or $C_3 + C_3$, and it may be consumed by forming C_7 (with C), C_8 (with C_2), and C_9 (with C_3), etc. In the general case, the kinetic equations may be written

$$d[C_n]/dt = \sum_{m=1}^{[n/2]} k_{m,n-m}[C_m][C_{n-m}] - \sum_{m=1}^{N+1-n} k_{n,m}[C_n][C_m], \tag{1}$$

where n is the number of carbons in the cluster under study and N is the number of carbons in the largest cluster considered here (i.e., 9). $[n/2]$ denotes the maximum integer in $n/2$. The first term (on the RHS) involves the formation of C_n via the bimolecular reaction of the smaller clusters C_m and C_{n-m} and the second term accounts for the reactions which deplete C_n to form larger clusters. Rather than use absolute concentrations of the cluster species, we introduce relative concentrations defined by

$$[C_n]^r = [C_n]/C_0,$$

where $C_0 \equiv \sum_{n=1}^{N} n[C_n] = \text{constant}$. Hence we find

$$d[C_n]^r/dt = C_0\left\{\sum_{m=1}^{[n/2]} k_{m,n-m}[C_m]^r[C_{n-m}]^r - \sum_{m=1}^{N+1-n} k_{n,m}[C_n]^r[C_m]^r\right\}. \tag{2}$$

This set of coupled equations requires certain assumptions and simplifications. We adopt the approach

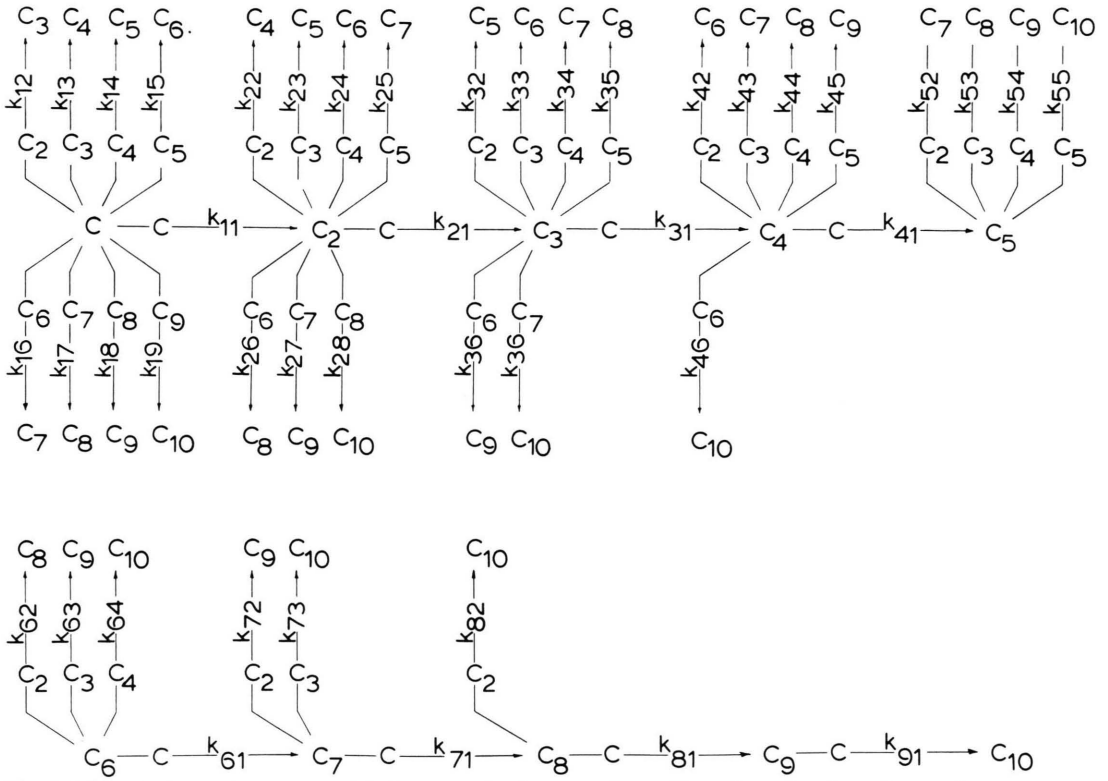

Fig. 5. The net of reactions assumed to be operative between thermally-activated carbon clusters in a rare gas matrix (for $n = 1$ to 10).

originally taken by Smoluchowski[12] and further developed by Waite[29]. In this approach, two species such as C_n and C_m react upon diffusion in a solid matrix. The kinetic equation for the process is given by

$$\mathrm{d}[C_n]/\mathrm{d}t = \mathrm{d}[C_m]/\mathrm{d}t = -k_{n,m}[C_n][C_m], \tag{3}$$

where

$$k_{n,m} = 4\pi R(D_n + D_m) \cdot (1 + R[\pi(D_n + D_m)t]^{-1/2}). \tag{4}$$

Here R is the radius of the reaction sphere, D_n and D_m are the diffusion coefficients (for C_n and C_m, respectively) and t is the diffusion time. We assume further that these diffusion coefficients are inversely proportional to the number of carbons in the cluster chain and directly proportional to a Boltzmann-like term involving the diffusional activation barrier, E_n. Thus, we have

$$D_n = n^{-1/2}\,\mathrm{D}_0 \exp(-E_n/RT). \tag{5}$$

Note the inverse square root dependence of D_n on n such that the diffusion rate is inversely proportional to the square root of the molecular weight. This inverse mass dependence reflects our expectation of lower D_n diffusion coefficients for higher mass clusters. Although it appears that all (small) cluster sizes can undergo diffusion we make the physically-reasonable assumption that the activation energy for diffusion varies linearly with cluster size. Thus

$$E_n = a + b(n-1), \tag{6}$$

where a and b are two activation parameters to be fit (*vide infra*). The influence of factors such as cluster size (volume) and shape on ability to diffuse through a matrix enter indirectly through the activation energy, E_n.

D_0 in (5) is estimated in the following manner from the diffusion coefficient for Cu atoms in solid argon[30]. Solid state theory relates the activation energy, E, for autodiffusional processes to temperature by

$$E \cong 0.032\ T_{\mathrm{MP}},\ \mathrm{kcal/mol}, \tag{7}$$

where T_{MP} is the melting point temperature. For Ar, $T_{\mathrm{MP}} = 83.8$ K, so $E_{\mathrm{Ar}} \cong 2.68$ kcal/mol. In this model it is assumed that E_{Ar} (in Ar) $\cong E_{\mathrm{Cu}}$ (in Ar) $\cong E_{\mathrm{C}}$ (in Ar).

We take the ratio of the C and Cu diffusion coefficients as

$$D_C/D_{Cu} = \sqrt{M_{Cu}/M_C} = 2.3, \quad (8)$$

where M_{Cu} is the atomic weight of Cu. Since $D_{Cu} = 4 \times 10^{-17}$ cm^2/s at 35 K in Ar,[30] $D_C = 9.2 \times 10^{-17}$ cm^2/s. Using this value and the above value for E_C in (5) yields D_0 (in Ar) $\cong 4.3$ cm^2/s. This value of D_0 is exactly equal to the average value obtained in two autodiffusional (self-diffusion) experiments for Ar crystals and films using a radioactive tracer-exchange method[31]. In these two experiments the activation energy for self-diffusion was found to be 3.8 kcal/mol.

C_0 in (2) is obtained by assuming a matrix ratio of Ar to C atoms of 200 to 1, and an Ar atom radius of 1.9 Å. This leads to $C_0 = 1.2 \times 10^{20}$ C atoms/cm^3. We take the reaction sphere radius (R) as 4 Å. In addition to the quantities discussed above, N initial concentrations $[C_N]^r$ ($t = 0$) are also required; they are subject to the normalization condition

$$\sum_n n[C_n]^r(t) = 1.$$

These relative concentrations are estimated initially from available theoretical intensities (transition moments)[32] and experimental intensity data. They are subsequently varied to effect the fit to experiment.

D) *Computational Approach*

Before discussing the computational approach taken, it is useful to briefly review the number and type of parameters in the model. First, there are a total of 25 rate constants in our treatment ($k_{1,1-9}$, $k_{2,2-8}$, $k_{3,3-7}$, $k_{4,4-6}$, and $k_{5,5}$), which are determined by 9 diffusion constants ($D_1 - D_9$) and the reaction sphere, R (cf. (4)). Thus, 25 rate constants are replaced by the latter 10 rate parameters. However, our assumption that the diffusion constants can be described with an diffusional activation energy which varies linearly with cluster size, reduces these 10 rate parameters to only 2, i.e. the a and b in (6). In addition, to solve the coupled equations in (2), we also require initial cluster concentrations. They are firstly chosen from theoretical intensities and experimental intensity data and then varied. In summary, we vary 11 parameters (two activation energy components and 9 concentrations) to effect the fit to 30 observational points (5 cluster band intensities each at 6 different temperatures).

To solve the system of coupled differential equations (2), a fourth-order Runge-Kutta algorithm with a fixed step size was employed[33]. The nine equations ($1 \leq n \leq 9$) of (2) were integrated as a function of time for six different fixed temperatures (12, 23, 30, 33, 36, and 38 K). For each temperature, integration was carried out for a period of 600 s (1000 0.6 s steps). Concentration ratios, $[C_n]^r_T/[C_n]^r_{12K}$, were determined because they are directly comparable to experimental intensity ratios, $I_n(T)/I_n(12\,K)$, since the transition moments cancel. The results of the calculation are shown in Fig-

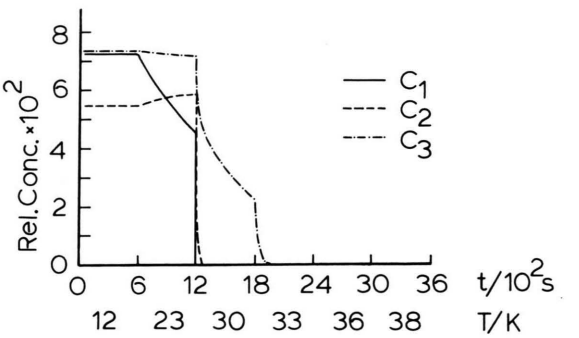

a) Profile for C_n ($n = 1$ to 3).

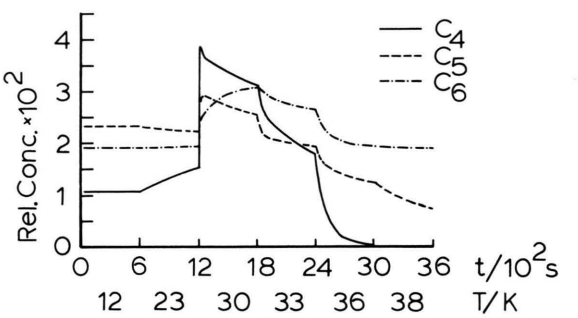

b) Profile for C_n ($n = 4$ to 6).

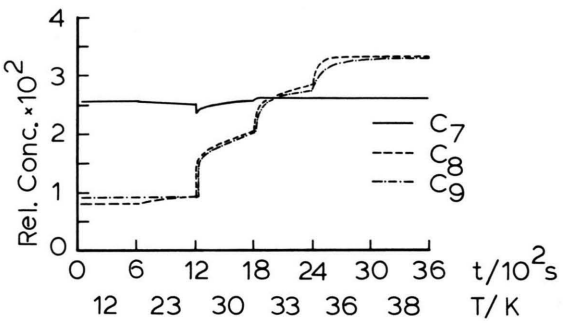

c) Profile for C_n ($n = 7$ to 9).

Fig. 6. Concentration profiles for the carbon clusters, C_n ($1 \leq n \leq 9$) as function of time (and temperature). The dual abscissa denotes that the matrix is at 12 K for the time span 0 to 600 s, at 23 K for the span 600 to 1200 s, etc.

Table 1. Initial Concentrations and Activation Energies for Linear Carbon Clusters, C_n, in Argon Matrices.

n	$100\,[C_n]^r\,(t=0)$	E_n^*
1	7.274	1.80
2	5.467	2.02
3	7.345	2.24
4	1.063	2.46
5	2.319	2.68
6	1.914	2.90
7	2.545	3.12
8	0.807	3.34
9	0.906	3.56

* $E_n = 1.8 + 0.22\,(n-1)$ kcal/mole.

ure 6. Two variables, time (t) and temperature (T), are plotted along the abscissa. Their interpretation is as follows: from 0 to 600 s, the concentration profiles ($[C_n]^r_T$ vs. t) are plotted for 12 K. Note that no change in $[C_n]^r$ is predicted for any species. At $t = 600$ s, T was raised "instantaneously" to 23 K and in the interval 600–1200 s the time evolution of $[C_n]^r$ plotted. In this time-temperature interval $[C_1]^r$ falls by ~50%, $[C_2]^r$ rises, while $[C_{3,5,6}]^r$ all decline slightly. At 1200 s the temperature is raised to 30 K where significant changes occur. $[C_{1,2}]^r$ drop precipitously to practically zero, $[C_3]^r$ declines strongly, while all the rest jump in concentration, $[C_4]^r$ by more than 300%. Similar advances in temperature to a maximum of 38 K influence the species differently and may be followed readily on the plot.

To obtain the theoretical points in Fig. 4, the relative concentrations, $[C_n]^r$, were taken at the end of each 600 s interval. This plot corresponds more closely to experiment since no time dependence is included; only the static concentrations (IR intensities) of the species after annealing at a particular temperature are recorded. Note that the curves have all been normalized to the concentrations/intensities at 12 K; thus all growth/decay curves start at an ordinate of 1.0. The fit to the known clusters is reasonably good. The optimized initial concentrations and activation energies found are presented in Table 1. Comparison of calculated and experimental intensity (relative concentration) ratios (i.e., $I_n(T)/I_n(12\text{ K})$) is given in Table 2. While some discrepancies are evident, the overall annealing trends mimic the experimental data rather well. The C_3 and C_5 species decay with increasing temperature with C_3 commencing at a lower temperature. The C_6 cluster grows to a maximum at ~33 K and declines thereafter, while C_9 climbs 400% up to ~36 K at which temperature it starts to level off. The unknown clusters are each predicted to behave differently. The C_7 chain is predicted to show little variation with temperature. On the other hand, C_4 is predicted to increase dramatically at 30 K and then drop off. C_8 is expected to increase quickly at 30 K and then gently increase with further temperature increases. Of the prominent unassigned IR bands the ones at 2128 cm^{-1} and 1894 cm^{-1} are observed to vary little with annealing temperature increase. We therefore assign them to the linear C_7 species.

V. Discussion

In this paper evidence has been presented on the aggregation of small carbon clusters upon annealing of the argon matrix in which they are trapped. It has been observed that the C_3 and C_5 clusters decay when the matrix is warmed while the C_6 and C_9 species grow. A kinetic reaction network which includes solid state diffusion of all possible pairwise combinations of small clusters ($1 \leq n \leq 10$) has been shown to account reasonably well for the growth/decay patterns of the known clusters. Activation energies for these aggregation steps have been extracted under the assumption that they increase linearly with cluster size. They all fall in the range 1.8 kcal/mol ($n = 1$) to 3.6 kcal/mol ($n = 9$). The fit to the growth/decay curves with temperature (cf. Fig. 4) mimics the experimental points rather well, with the exception of C_3: its fit falls off much faster with temperature than observed. This may result from a too-small activation energy. The calculational results are very sensitive to the activation energies chosen. If the assumed linear form for the activation energy is not applicable to the C_3, this could result in a erroneously small energy barrier and a reaction which progresses too rapidly.

In addition to the fit to the known clusters, the results also yield predicted profiles for the unassigned clusters (i.e., those clusters whose vibrational frequencies are forbidden (C_2) or, as yet, not conclusively determined (C_7, C_8)). The predictions are given in Table 3 (and for C_7 in Table 2 also). Interestingly, the prediction for C_8 closely parallels that for C_9 (cf. Figure 6).

The most significant prediction which emerges from the calculations concerns the C_7 clusters. It may be seen in Fig. 6 that its concentration is predicted to vary negligibly over the 12–38 K temperature range.

Table 2. Experimental and Theoretical (in parentheses) Intensity Ratios, $I_n(T)/I_n(12\,K)$, for Various Carbon Clusters[a].

T/K	$t/10^2$ s	C_3 2039 cm^{-1}	C_5 2164 cm^{-1}	C_6 1952 cm^{-1}	C_7 2128 cm^{-1}	C_9 1998 cm^{-1}
12	0–6	1.00 (1.00)	1.00 (1.00)	1.00 (1.00)	1.00 (1.00)	1.00 (1.00)
23	6–12	0.95 (0.98)	1.01 (0.97)	1.02 (1.01)	1.06 (0.98)	1.22 (1.16)
30	12–18	0.79 (0.31)	0.82 (1.10)	1.11 (1.62)	1.12 (1.01)	2.57 (2.52)
33	18–24	0.52 (0.00)	0.56 (0.84)	1.18 (1.40)	1.12 (1.03)	4.05 (3.52)
36	24–30	0.27 (0.00)	0.44 (0.54)	1.12 (1.02)	1.12 (1.03)	4.00 (4.13)
38	30–36	0.14 (0.00)	0.31 (0.32)	0.94 (1.01)	1.06 (1.03)	4.00 (4.13)

[a] Experimental data for the clusters C_3, C_5, C_6, C_7, and C_9 were used in the fit (see text). RMS Error = 0.24.

Table 3. Theoretical Intensity Ratios, $I_n(T)/I_n(12\,K)$ for C_1, C_2, C_4, C_7, and C_8[a].

T/K	$t/10^2$ s	C_1	C_2	C_4	C_7	C_8
12	0–6	1.00	1.00	1.00	1.00	1.00
23	6–12	0.63	1.08	1.45	1.06	1.00
30	12–18	0.00	0.00	2.95	1.12	2.23
33	18–24	0.00	0.00	1.69	1.12	3.03
36	24–30	0.00	0.00	0.04	1.12	3.62
38	30–36	0.00	0.00	0.00	1.06	3.64

[a] RMS error = 0.24 for fit to C_3, C_5, C_6, C_7, and C_8; note that $I_n(T)/I_n(12\,K) = [C_n]^r_{(T)}/[C_n]^r_{(12\,K)} = [C_n]_{(T)}/[C_n]_{(12\,K)}$.

Of the major bands in the C–C stretch region, only the 2128 cm^{-1} and 1894 cm^{-1} bands are observed to display this independence of temperature. On the basis of this similarity we assign these two bands to the linear C_7 cluster. As mentioned in Sect. IIIF, Saykally and co-workers[24] have recently assigned a gas phase band at 2138 cm^{-1} to linear C_7. The 10 cm^{-1} gas-to-matrix shift for the 2128 cm^{-1} band is larger than the 5 cm^{-1} gas-to-matrix seen for C_5, but is still only a 0.5% shift, a not unreasonable value[34]. Finally, Martin, Francois and Gijbels[23] have argued persuasively on theoretical grounds that the 2128 cm^{-1} band should be assigned to linear C_7.

Acknowledgements

We gratefully acknowledge the National Science Foundation for its support of this research under Grant No. CHE-8903133. We also thank Dr. J. M. L. Martin for a preprint of his work before publication.

[1] For a recent review, see W. Weltner, Jr. and R. Van Zee, Chem. Rev. **89,** 1713 (1989).
[2] K. R. Thompson, R. L. DeKock, and W. Weltner, Jr., J. Amer. Chem. Soc. **93,** 4688 (1971).
[3] W. Krätschmer and K. Nachtigall, in *Polycyclic Aromatic Hydrocarbons and Astrophysics*, eds. A. Léger, L. d'Hendecourt and N. Boccara, D. Reidel Publishing Co., Dordrecht 1987.
[4] M. Vala, T. M. Chandrasekhar, J. Szczepanski, and R. Pellow, in *Materials Chemistry at High Temperature*, Vol. II, ed. J. Hastie, Humana Press, 1990; and High Temperature Science **27,** 19 (1990).
[5] J. Kurtz and D. Huffman, J. Chem. Phys. **92,** 30 (1990).
[6] I. Yamada, H. Usui, and T. Takagi, in *Metal Clusters*, Eds. F. Träger and G. zu Putlitz, Springer-Verlag, Berlin 1986, p. 37ff.
[7] A. W. Castleman, Jr. and R. G. Keesee, ibid, p. 67ff.
[8] a) J. Bernholc and J. C. Phillips, J. Chem. Phys., **85(6),** 3258 (1986); b) J. Bernholc and J. C. Phillips, Phys. Rev. B, **33,** 7395 (1986).
[9] G. A. Ozin and H. Huber, Inorg. Chem. **17,** 155 (1978).
[10] M. Moskovits and J. E. Hulse, J. Chem. Soc. Faraday Trans. 2 **73,** 471 (1977).
[11] T. Nishiya, N. Hirota, H. Shinohara, and N. Nishi, J. Phys. Chem. **89,** 2260 (1985).
[12] a) M. V. Smoluchowski, Z. Phys. Chem. **92,** 192 (1917); b) cf. S. Chandrasekhar, Rev. Mod. Phys. **15,** 1 (1943).
[13] J. Szczepanski and M. Vala, J. Phys. Chem. **95,** 2792 (1991).
[14] R. J. Van Zee, R. F. Ferrante, K. J. Zeringue, and W. Weltner, Jr., J. Chem. Phys. **88,** 3465 (1988).
[15] W. Weltner, Jr., P. N. Walsh, and C. L. Angell, J. Chem. Phys. **40,** 1299 (1964).
[16] W. Weltner, Jr. and D. McLeod, Jr., J. Chem. Phys. **40,** 1305 (1964).
[17] L. N. Shen and W. R. M. Graham, J. Chem. Phys. **91,** 5115 (1989).
[18] M. Vala, T. M. Chandrasekhar, J. Szczepanski, Richard Van Zee, and W. Weltner, Jr., J. Chem. Phys. **90,** 595 (1989).
[19] R. Pellow and M. Vala, Z. Physik D **15,** 171 (1990).
[20] a) N. Moazzen-Ahmadi, A. R. W. McKellar, and T. Amano, Chem. Phys. Lett. **157,** 1 (1989); b) J. R. Heath, A. L. Cooksey, M. H. W. Gruebele, C. A. Schuttenmaer, and R. J. Saykally, Science **244,** 564 (1989).
[21] P. F. Bernath, K. H. Hinkle, and J. J. Keady, Science **244,** 562 (1989).
[22] M. Vala, T. M. Chandrasekhar, J. Szczepanski, and R. Pellow, J. Mol. Structure **222,** 209 (1990).

[23] J. M. L. Martin, J. P. Francois, and R. Gijbels, J. Chem. Phys. **93,** 8850 (1990).
[24] J. R. Heath, R. A. Sheeks, A. L. Cooksy, and R. J. Saykally, Science **249,** 895 (1990).
[25] a) J. R. Heath and R. J. Saykally, J. Chem. Phys. **93,** 8392 (1991); b) J. R. Heath and R. J. Saykally, J. Chem. Phys. **94,** 1724 (1991).
[26] J. Szczepanski, R. Pellow, and M. Vala, in preparation.
[27] K. S. Pitzer and E. Clementi, J. Amer. Chem. Soc. **81,** 4477 (1959).
[28] W. R. M. Graham, K. I. Dismuke, and W. Weltner, Jr. Astrophys. J. **204,** 301 (1976).
[29] T. R. Waite, Phys. Rev. **107**(2), 463 (1957).
[30] M. Moskovits and G. A. Ozin in *Cryochemistry*, eds. M. Moskovits and G. A. Ozin, Wiley-Intersci., New York 1976, p. 335.
[31] A. V. Chadwick, in *Mass Transport in Solids*, eds. F. Bénière and C. R. A. Catlow, NATO ASI Series B: Physics, **97,** 309 (1981).
[32] J. Kurtz and L. Adamowicz, Astrophys. J. **370,** 784 (1991).
[33] W. H. Press, B. P. Flannery, S. A. Teukolsky, and W. T. Vetterling, *Numerical Recipes*, Cambridge University Press, London 1989, p. 550.
[34] M. E. Jacox, Rev. Chem. Intermed. **2,** (1) 1–36 (1978).